Journal Pre-proofs

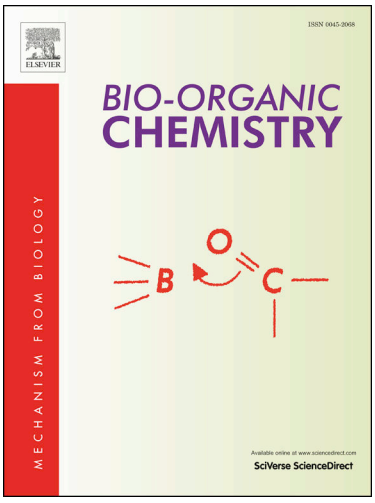

Click chemistry synthesis, biological evaluation and docking study of some novel 2'-hydroxychalcone-triazole hybrids as potent anti-inflammatory agents

Andrew N. Boshra, Hajjaj H.M. Abdu-Allah, Anber F. Mohammed, Alaa A. Hayallah

PII: S0045-2068(19)31829-2
DOI: https://doi.org/10.1016/j.bioorg.2019.103505
Reference: YBIOO 103505

To appear in: *Bioorganic Chemistry*

Received Date: 29 October 2019
Revised Date: 26 November 2019
Accepted Date: 10 December 2019

Please cite this article as: A.N. Boshra, H.H.M. Abdu-Allah, A.F. Mohammed, A.A. Hayallah, Click chemistry synthesis, biological evaluation and docking study of some novel 2'-hydroxychalcone-triazole hybrids as potent anti-inflammatory agents, *Bioorganic Chemistry* (2019), doi: https://doi.org/10.1016/j.bioorg.2019.103505

Click chemistry synthesis, biological evaluation and docking study of some novel 2'-hydroxychalcone-triazole hybrids as potent anti-inflammatory agents

Andrew N. Boshra[a], Hajjaj H. M. Abdu-Allah[a*], Anber F. Mohammed[a], Alaa A. Hayallah[ar,*]

[a] Department of Pharmaceutical Organic Chemistry, Faculty of Pharmacy, Assiut University, Assiut 71526, Egypt

Prof. Dr. Alaa Hayallah

Tel. 002-088-2411312 (office.) Fax. 002-08088-332776. alaa_hayalah@yahoo.com

Dr. Hajjaj Abdu-Allah

Work: (+2088)240-1521 Mobile: +201010211566 hajjaj@aun.edu.eg

ORCID: 0000-0002-4474-9086

[r]Present address: Department of Pharmaceutical Chemistry, Faculty of Pharmacy, Deraya University, El-Minia, Egypt.

Abstract

A hybrid pharmacophore approach is used to design and synthesize two novel series of 2'-hydroxychalcone-triazole hybrid molecules **6a-j** and **8a-j**. These compounds were fully characterized by spectral and elemental analyses. They were evaluated *in vitro* and *in vivo* for anti-inflammatory activity. Most of compounds were selective inhibitors for COX-2. Among them, compounds **6d**, **6f**, **6i**, **8c**, **8e** and **8h** demonstrated highly potent dual inhibition of COX-2 (IC_{50} = 0.037-0.041 μM) and 15-LOX (IC_{50} = 1.41-1.80 μM). Compounds **6i**, **8c** and **8h** showed 116%, 113% and 109% of the *in vivo* anti-inflammatory activity of celecoxib. Therefore, compounds **6d**, **6f**, **6i**, **8c**, **8e** and **8h-j** are potent dual inhibitor of COX-2 and 15-LOX. Docking study over COX-2 and 15-LOX active sites ensures the binding affinity and selectivity. These compounds are promising candidates for further development as anti-inflammatory drugs.

Keywords: Chalcone; Fries Rearrangement; Click; Triazole; Isatin; COX-2; 15-LOX; Anti-inflammatory

1. Introduction

Inflammation not only mitigates infections, initiates tissue repair and regeneration but it also causes many chronic and degenerative diseases [1]. It occurs due to stimulation of various cyclooxygenase (COX) and lipoxygenase (LOX) isozymes to produce inflammatory mediators like prostaglandins (PGs) and leukotrienes. The various symptoms of inflammation include heat, swelling, redness, pain, and loss of function of body parts such as imbalances in the movements of limbs. Other signs result in an increase in the number of white blood cells, fibrinogen and serum amyloid A protein (SAA), presence of C-reactive proteins (CRP), and fever [2]. Non-steroidal anti-inflammatory drugs (NSAIDs) are the most frequently used treatment for inflammatory symptoms. Their activities result from inhibition of cyclooxygenase (COX) mediated production of pro-inflammatory prostaglandins and thromboxanes [3]. However, long-term therapy with NSAIDs is usually accompanied by undesirable side effects on the gastrointestinal, renal, hepatic, and cardiovascular systems [4]. Therefore, the discovery of new NSAIDs with better safety profiles remains an active area of research. Chalcone moiety has found to be such a privileged pharmacophore in many biologically active compounds and continue to be of great interest to researchers owing to its promising applications in medicinal chemistry [5]. Several natural and (semi-) synthetic chalcones have demonstrated anti- inflammatory activity through inhibition of COX, prostaglandin E_2, inducible NO synthase, nuclear factor κB activities and tumor necrosis factor-α (TNF- α) [6]. For example, 2'-hydroxylated chalcones showed anti-inflammatory activity through LOX inhibition [7], while 3,4-dihydroxychalcones showed dual inhibition of COX-2 and 5-LOX [8]. 3-(pyridine-4-yl)-1H-pyrazole-5-carboxamide chalcones exhibited both anti-inflammatory and antioxidant activity [9]. On the other hand, many isatin derivatives have been synthesized and tested for their anti-inflammatory activity and showed promising results. 3-Thiosemicarbazino isatin [10], phenylhydrazone of isatins [11] exhibited good anti-inflammatory activity, also, ring substituted isatin showed good inhibitory activity to COX-2 [12]. Furthermore, numerous evidences in scientific literature advocate the 1,2,3-triazole efficacy in context of inflammation and analgesia [13-15]. Their ability to intervene in the selective COX-2 inhibition and inhibiting the 5-LOX enzyme is said to be the cardinal factor associated with their anti-inflammatory potential [13-15]. Moreover, 1,2,3-triazole tethered indole-3-glyoxamide derivatives have been designed as dual inhibitors of COX-2 and 5-LOX for cancer chemotherapy [16]. Combining bioactive pharmacophores to design a hybrid molecule is a useful tool to generate lead molecules with synergetic biological activities and superior efficacy [17]. Recently, increasing evidence indicates that

simultaneous modulation of multiple targets may improve both therapeutic safety and efficacy, compared with single-target drugs [18]. Taking into consideration the aforementioned information and as a continuation of our project on searching for new biologically active hybrids [19-22], we envisaged that chalcone, 1,2,3-triazole and isatin pharmacophores if linked together would generate hybrid molecules with good and broad-spectrum anti-inflammatory activities through selective inhibition of COX-2 and LOX.

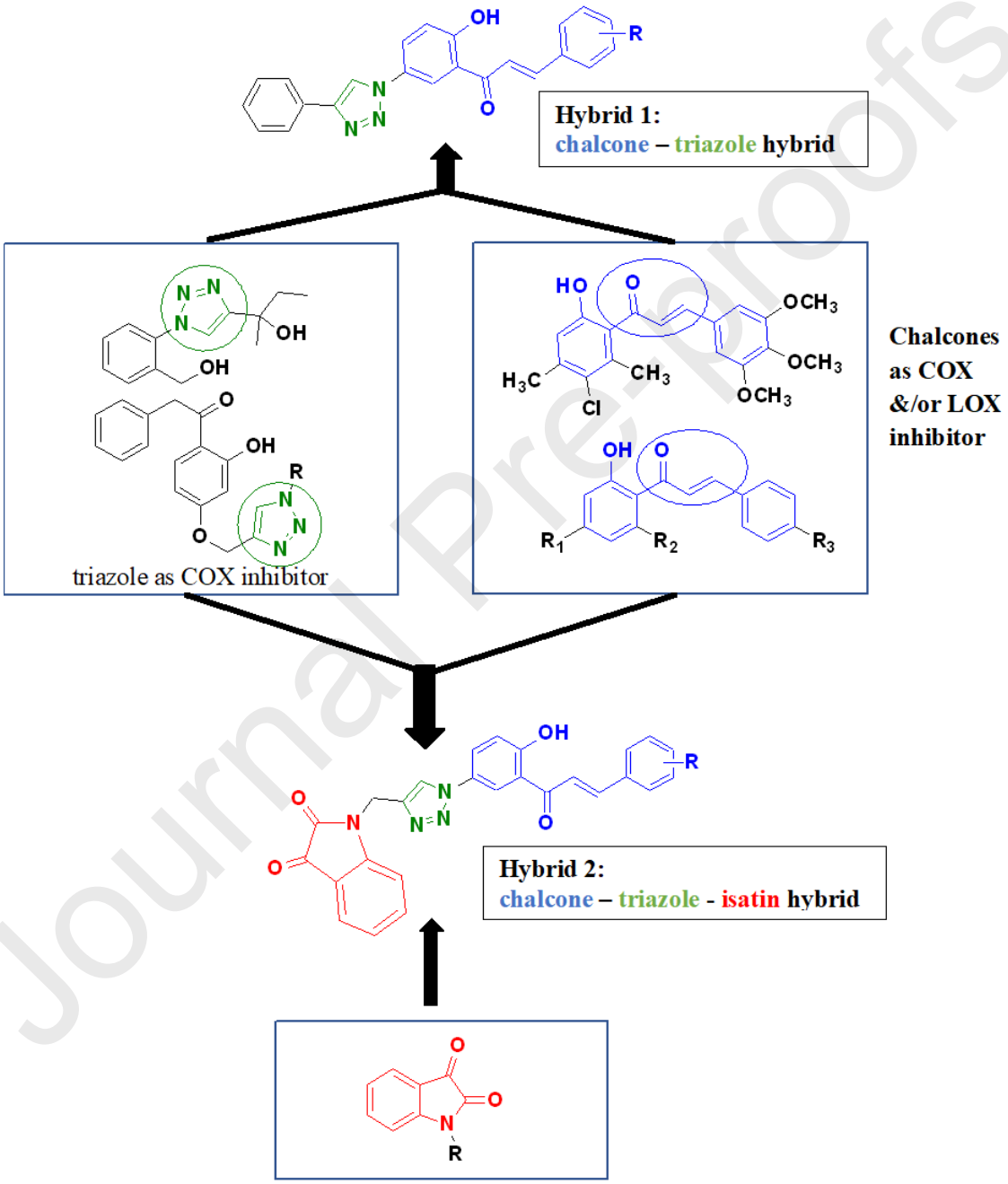

Fig. 1. The design strategy for chalcone–triazole hybrids.

Moreover, varied substituents were introduced to C-4 of phenyl of chalcone in order to explore their electronic and/or steric effects and contribution to the activity. This strategy could afford new molecules with multitarget and improved anti-inflammatory activity profiles. The design strategy for chalcone-triazole hybrids is shown in Fig. 1.

2. Results and discussion

2. 1. Chemistry

The target compounds **6a-j** and **8a-j** were synthesized as depicted in Schemes (1 and 2) starting from the key intermediate **4**. *p*-Aminophenol was considered a proper starting material for the synthesis of **4** by azidation, phenolic acetylation followed by Fries rearrangement. However, product from azidation was semisolid and difficult to purify. Alternatively, *p*-anisidine was used. It was *N*-acetylated by reaction with acetic anhydride. The acetylated compound was subjected to Friedel-Crafts acetylation by reaction with acetyl chloride in presence of $AlCl_3$. As expected, under these condition methoxy ether bond was cleaved to give phenolic OH which directly acetylated to give phenyl acetate ester that undergone Fries rearrangement to give compound **2**, since the *p*-position is occupied**.** Acidic hydrolysis of **2** gave 5-amino **3**. Diazotization of **3** followed by azide substitution furnished 5-azido-2-hydroxyacetophenone **4**. The structure of **4** was verified by the disappearance of NH_2 hump at δ 3.30 in ^{1}H NMR and confirmed by the azide peak at 2113 cm^{-1} in IR. The synthesis of **4** starting from *p*-anisidine afforded high yield (90%), it was scalable, and all produced intermediates are crystallizable. Synthesis of this compound was reported recently starting from **3** [23]. In this study the work-up was modified to a simple procedure, the reaction mixture was gradually cooled without neutralization and the product recrystallizes in analytically pure form in excellent yield. Thus, this is a completely green step devoid of any organic solvents in the reaction as well as work up. Aldol condensation of **4** with un/substituted benzaldehydes and cinnamaldehyde provided ten azido chalcone derivatives **5a-j** (Scheme 1)**.** Click reaction between **5a-j** and phenyl acetylene gave chalcone–phenyltriazole hybrids **6a-j** (Scheme 2). On the other hand, click reaction of **5a-j** with *N*-propargylisatin **7** [24] provided the second series **8a-j** (chalcone–triazole–isatin hybrids) (Scheme 2). All compounds were characterized by NMR and IR. All final compounds (**6a-j** and **8a-j**) were confirmed further by elemental analyses. ESI-MS was measured for compounds **6a** and **6b**.

The chemical structures of compounds **5a-j** were verified by the appearance of C=O band at 1644 cm^{-1} in IR, while ^{1}H NMR showed two protons of alkene appear in the aromatic region

at δ 7.7 and δ 7.9 ppm. ^{1}H NMR spectra of all final compounds (**6a-j** and **8a-j**) showed the triazole proton resonated as a singlet at *δ* around 8.4 ppm.

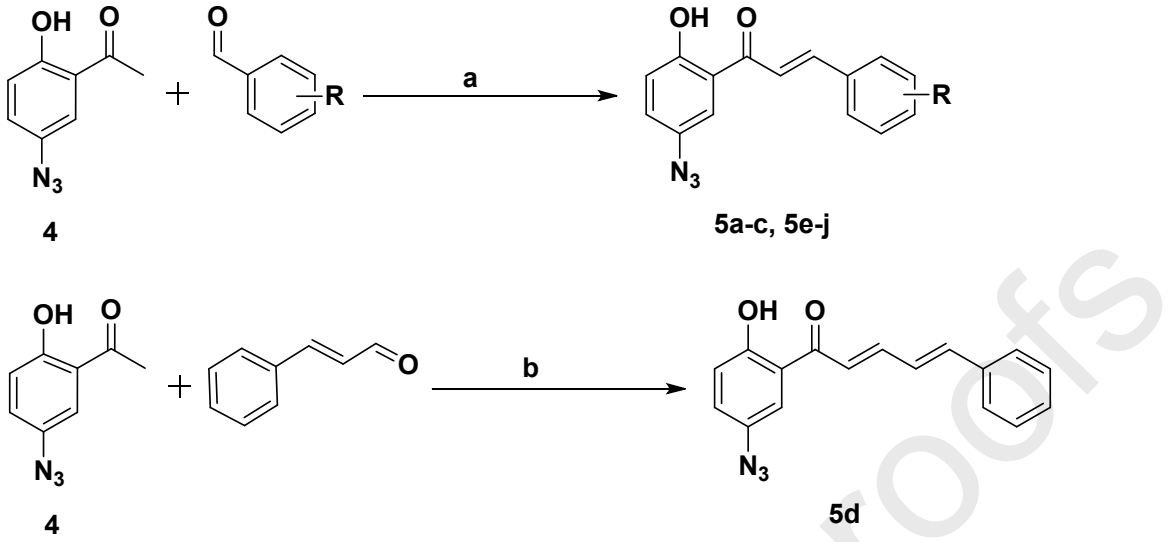

Scheme 1. Reagents and conditions: (a) NaOH-ethanol, 0.5-12 h, 50-70% yield; (b) NaOH-ethanol, 1h, 60% yield.

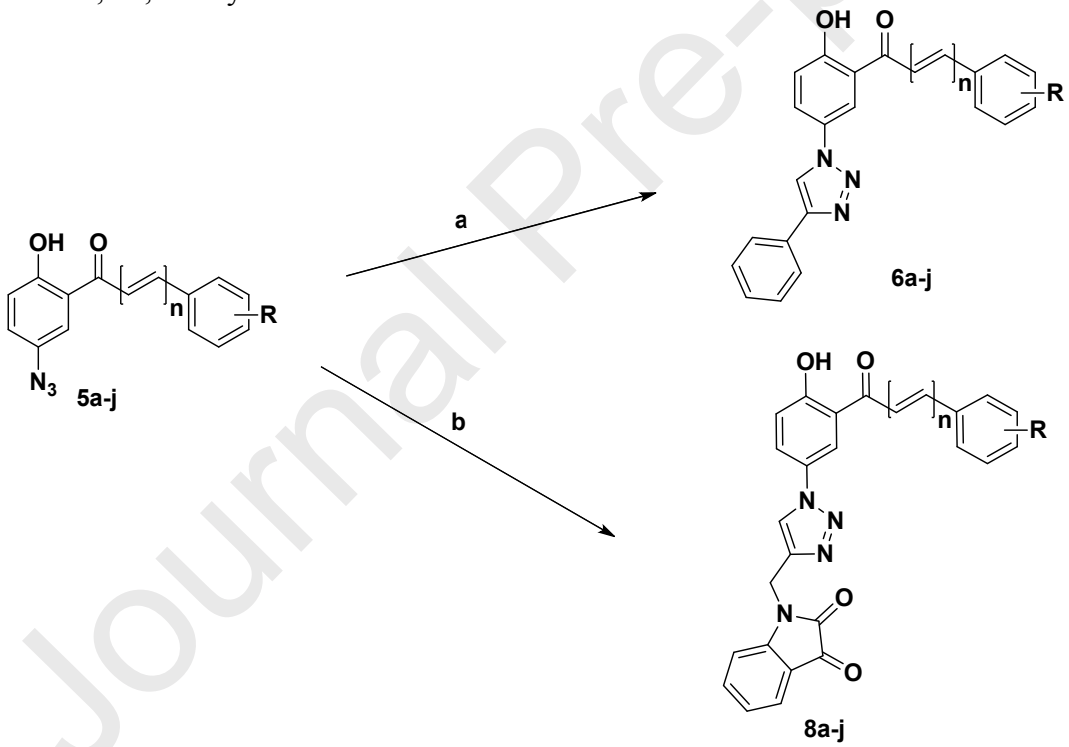

Scheme 2. Reagents and conditions: (a) phenylacetylene, $CuSO_4$, sod. ascorbate, *t*-butanol-water, 70-80 °C, 12-24 h. (b) *N*-propargylisatin, $CuSO_4$, sod. ascorbate, *t*-butanol-water, 70-80°C, 12-24 h.

Compd. no.	R	n	Compd. no.	R	n
5a, **6a**, **8a**	H	1	**5f**, **6f**, **8f**	4-Cl	1
5b, **6b**, **8b**	4-Me	1	**5g**, **6g**, **8g**	4-OH	1

5c, **6c**, **8c**	4-DMA	1	**5h**, **6h**, **8h**	4-OMe	1
5d, **6d**, **8d**	H	2	**5i**, **6i**, **8i**	3,4-$(OMe)_2$	1
5e, **6e**, **8e**	4-Br	1	**5j**, **6j**, **8j**	3,4,5-$(OMe)_3$	1

2.2. Biology

2.2.1. *In vitro* Cyclooxygenase inhibition.

All final compounds (**6a-j, 8a-j**) were tested for their inhibitory potencies against ovine COX-1 and human recombinant COX-2. Celecoxib and Indomethacin (INM) were taken as standards. The results are shown in (Table 1). All tested compounds displayed higher inhibitory potency against COX-2 (IC_{50} = 0.037- 0.23 µM) than COX-1 (IC_{50} = 7.4-13.7 µM) with COX-2 selectivity indexes (COX-1 IC_{50} /COX-2 IC_{50}) in the range of 32.17-360.53.

Table 1.

COX and 15-LOX inhibitory potencies and selectivity indexes of compounds **6a-j**, **8a-j** and reference drugs

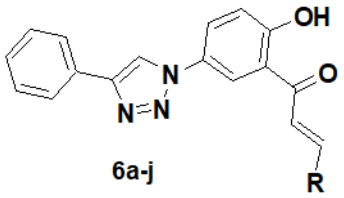

6a-j

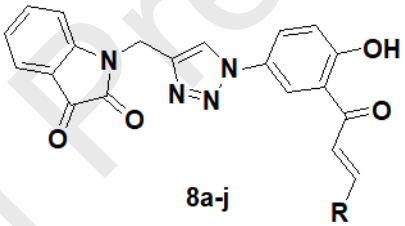

8a-j

Compd. No.	R	COX-1 IC_{50}[a] (µM)	COX-2 IC_{50}[a] (µM)	Selectivity index[b] (SI)	15-LOX IC_{50}[a] (µM)
Celecoxib	-	14.7	0.045	326.67	-
Indomethacin	-	0.041	0.51	0.08	-
Zileuton	-	-	-	-	15.6
6a	Ph	7.4	0.23	32.173	4.12
6b	4-CH_3Ph	9.8	0.11	89.09	5.11
6c	4-$(CH_3)_2$NPh	10.5	0.074	141.89	4.52
6d	-CH=CHPh	11.3	0.061	185.25	2.97
6e	4-BrPh	12.3	0.041	300	3.12
6f	4-ClPh	13.1	0.041	319.51	1.78
6g	4-HOPh	9.8	0.11	89.09	2.97
6h	4-CH_3OPh	7.9	0.12	65.83	3.98
6i	3,4-$(CH_3O)_2$Ph	12.4	0.052	238.46	1.68
6j	3,4,5-$(CH_3O)_3$Ph	10.9	0.068	160.29	2.11
8a	Ph	13.11	0.045	291.33	2.4
8b	4-CH_3-Ph	11.9	0.039	305.13	2.67
8c	4-$(CH_3)_2$N-Ph	13.4	0.043	311.63	1.58

8d	-CH=CHPh	11.5	0.087	132.18	2.14
8e	4-BrPh	13.7	0.038	360.53	1.41
8f	4-ClPh	10.9	0.11	99.09	3.97
8g	4-HOPh	9.9	0.091	108.79	3.45
8h	4-CH_3OPh	13.3	0.037	359.46	1.95
8i	3,4-$(CH_3O)_2$Ph	12.8	0.047	272.34	1.67
8j	3,4,5-$(CH_3O)_3$Ph	12.4	0.048	258.33	1.56

[a] IC_{50} value represents the concentration of the compound that produce 50% inhibition of COX-1, COX-2 or 15-LOX which is the mean value of two determinations where the deviation from the mean is < 10% of the mean value.[b] Selectivity index (COX-1 IC_{50} /COX-2 IC_{50}).

Results for COX-1 inhibition indicated that all tested compounds of phenyltriazole series (**6a-j**) exhibited comparable inhibitory potency (IC_{50} = 7.4–13.3 μM) to celecoxib (IC_{50} = 14.7 μM). On the other hand, all tested compounds showed high inhibitory profiles (IC_{50} = 0.037- 0.23 μM) against COX-2. Six compounds of this series, **6c, 6d-f, 6i** and **6j** exhibited high potency and selectivity comparable to the standard drug Celecoxib. Particularly, compounds **6e, 6f** and **6i** are equipotent to Celecoxib (IC_{50} = 0.045 μM) and more potent than INM (IC_{50} = 0.51 μM). The results showed that introducing electron donating group such as 3,4-dimethoxy (**6i;** IC_{50} = 0.052 μM) or electron withdrawing group such as 4-Br (**6e;** IC_{50} = 0.041 μM)) to the phenyl derivative (**6a;** IC_{50} = 0.23 μM) improved the potency. Particularly, introducing lipophilic moiety as Cl or Br increases inhibitory potency (IC_{50} = 0.041 μM)) as well as selectivity (SI = 319.5) against COX-2. In order to investigate the effect of phenyltriazole moiety on activity, phenyl group was replaced by isatin to give compounds (**8a-j**). Interestingly, some compounds (**8a, 8b** and **8h**) of this series showed higher potency and selectivity for COX-2 than the corresponding **6a, 6b an 6h**. While compounds **8c, 8e, 8i** and **8j** are slightly more potent and selective for COX-2 than the corresponding **6c, 6e, 6i** and **6j** as shown in Table 1. This improvement in potency of **8a-j** series may be attributed to the synergistic effect of isatin moiety. In contrast, compound **8f** showed dramatic decrease in potency and selectivity if compared to **6f**.

2.2.2. *In vitro* lipoxygenase inhibition

All final compounds (**6a-j**, **8a-j**) were evaluated for their ability to inhibit 15-LOX enzyme. Zileuton was taken as standard. The results are shown in Table 1. The compounds exhibit a range of potency IC_{50} 1.41-5.11 μM higher than Zileuton (IC_{50} = 15.6 μM). Several compounds (**6d**, **6e**, **6f**, **6g**, **6i** and **6j**) of phenyltriazole series showed high potency. Moreover, compounds 6f and 6i displayed promising potency with IC_{50} 1.78 and 1.68 μM respectively. Accordingly, compound **6f** and **6i** showed excellent dual inhibition of COX-

2/15-LOX and high selectivity. Similarly, isatin series (**8a-j**) showed higher potency than Zileuton. Among these compounds, compounds **8e** and **8h** has promising dual inhibition of both COX-2 and 15-LOX.

2.2.3. *In vivo anti-inflammatory activity*

The most potent compounds in *in vitro* studies (**6e, 6f, 6i, 8b, 8e** and **8h**) were screened for *in vivo* anti-inflammatory study by carrageenan induced paw edema bioassay in rats using celecoxib as a reference drug. The test compound was administrated *i.p.* at a dose of 28 μM/kg and the % of edema inhibition was calculated. The results (Table 2) revealed that most of the tested compounds showed a gradual increase of the anti-inflammatory activity up to its maximum effect after 3 h, while compounds **6e** and **8e** maintain this activity up to 5 h.

Table 2.

In vivo anti-inflammatory in rats using celecoxib as reference drugs

Compd No.	% of edema inhibition ± SE				
	1h	2 h	3 h	4 h	5 h
Celecoxib	44.0 ± 7.99	34.7 ± 7.53	61.2 ± 11.36	54.5 ± 5.25	62.8 ± 2.85
6e	38.6 ± 2. 12[c]	40.1 ± 2.72[c]	60.5 ± 2.8[d]	59.0 ± 3.11[d]	59.5 ± 2.10[c]
6f	38.0 ± 4.00[c]	42.4 ± 3.25[c]	62.5 ± 3.18[c]	61.1 ± 4.16[d]	58.1 ± 2.1[d]
6i	40.0 ± 6.93[b]	58.7 ± 7.84[d]	71.4 ± 4.08[d]	69.7 ± 3.03[d]	52.8 ± 2.47[d]
8b	39.8 ± 3.24[b]	52.6 ± 2.33[b]	59.3 ± 3.70[a]	60.3 ± 1.92[d]	59.1 ± 2.19[c]
8e	38.0 ± 3.10[c]	45.1 ± 3.34[d]	69.2 ± 3.27[d]	68.2 ± 2.60[a]	64.2± 2.11[b]
8h	40.2 ± 3.24[a]	41.14 ± 2.34[c]	66.5 ± 2.01[c]	64.1 ± 3.22[d]	60.4 ± 2.16[b]

[a] Significant difference at $P < 0.05$, [b] Significant difference at $P < 0.01$, [c] Significant difference at $P < 0.001$, [d] Significant difference at $P < 0.0001$.

The results are going well with that from *in vitro* studies. The structure activity relationship studies for the anti-inflammatory effects of triazole derivatives **6a-j** and **8a-j** shown in Tables 1 and 2 illustrated that the compounds that showed anti-inflammatory activities are not only contained electron-withdrawing substituents (**6e, 6f, 8e** and **8f**), but also electron-donating substituents on the phenyl moiety (**6i**). Of compounds with electron-withdrawing with halogen atom substituent groups, the introduction of Cl (**6e** and **8e**), or Br (**6f** and **8f**) at the *p*-position of the phenyl ring, resulted in the best anti-inflammatory activity, with the best

compounds being **8e** and **8h.** Both, in addition to **6i**, were the most active compounds with activity higher than celecoxib after 3 h. They showed 116%, 113% and 109% of the anti-inflammatory activity of celecoxib at 3 h interval. To rationalize the biological results at the molecular level docking studies were undertaken.

2.2.4. Docking study

Docking simulations of the new compounds (**6a-j** and **8a-j**) were performed using Molecular Operating Environment (MOE) software [25] and the crystal structures of rofecoxib bound to human cyclooxygenase-2 (PDB: 5KIR) [26] as well as human 15-Lipoxygenase-2 bound to a competitive inhibitor C_8E_4 (PDB: 4NRE) [27].

2.2.4.1. Docking to COX-2

Docking was performed and compared with three COX-2 inhibitors; indomethacin, celecoxib and rofecoxib to rationalize the biological results of the new compounds. Visualization of the active site revealed that COX-2 pocket is predominately lipophilic with several regions of hydrophilicity. Moreover, docking results revealed that celecoxib and indomethacin probe the space of the enzyme active site showing different binding modes (Table S1) that were found to be compatible with literature [28]. Coxibs such as celecoxib and rofecoxib adopt a binding pose within the COX-2 channel with their sulfone moiety inserted into the side pocket near Arg513. On the other hand, indomethacin forms a salt bridge between the ligand carboxylate moiety and the guanidinium moiety of Arg120 at the hydrophilic mouth of the active pocket. The remaining contacts for both selective and non-selective COX-2 inhibitors are hydrophobic in nature with Leu352, Ser353, Val349, Tyr355, Val523, Ala527.

Among the first series **6a-j**, the highly potent halogen substituted derivatives **6e** and **6f** were the best docked within the active site although they showed different orientations. They showed collective binding interactions for the known COX-2 inhibitors within the active site. The bulky bromo substituted phenyl of compound **6e** occupies the side pocket forming hydrophobic interactions with Val523, Leu352 and Ser353 as well as a CH-π interaction between the ligand triazole and Ala527 of the hydrophobic pocket (Table S1), while its carbonyl accepts a hydrogen bond interaction from Arg120 (Fig. 2A). Whilst compound **6f** is being upturned with its phenyl triazole moiety inserted in the side pocket forming hydrophobic interactions with Val523 and Leu352 as well as a hydrogen bond interaction with Ser353. In addition, the chloro group accepts a hydrogen bond interaction from Arg120 (Fig. 2B).

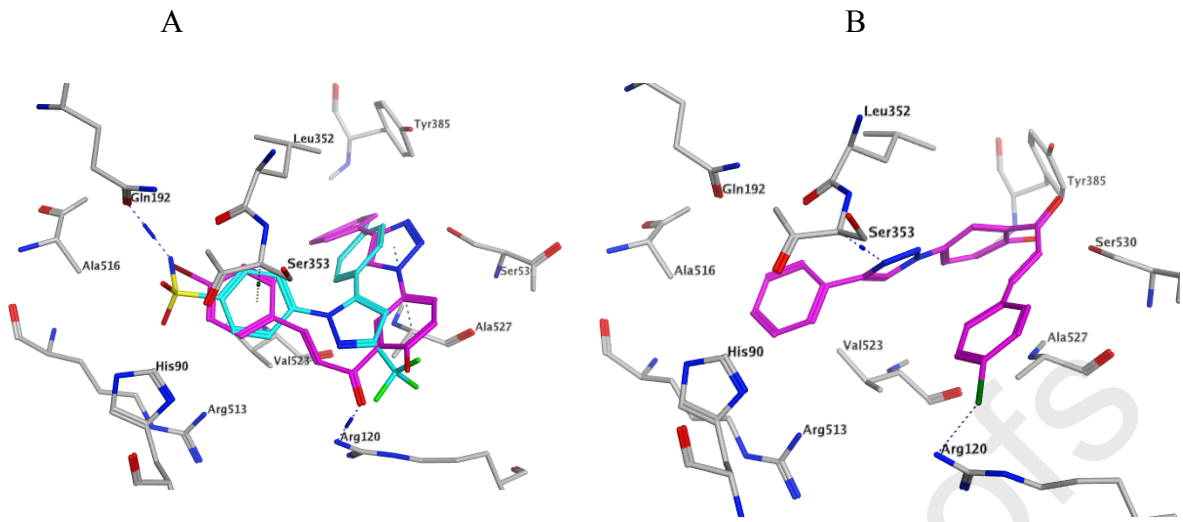

Fig. 2. Docking of compounds **6e** (purple) (A) aligned with celecoxib (cyan) and **6f** (B) into the COX-2 active site showing their orientations and binding modes.

The methoxy substituted derivatives **6g-6j** were found to exhibit an orientation similar to that of the chloro substituted compound. However, the position and/or number of the methoxy groups have an impact on the ring slope near Arg120. Compounds **6h** and **6j** showed weaker binding with their distant *p*-methoxy or bulky di *m*-methoxy groups. However, the moderately active compound **6i** showed better binding with its single *m*-methoxy group accepting a hydrogen bond interaction from Arg120. Also, the size of the hydrogen bond forming group affected the binding of the compound, the small hydroxyl group of **6g** failed to form a hydrogen bond interaction with Arg120 compared with the methoxy substituted compound **6i**.

The compound **6c** substituted with the basic dimethylamino group prefers to get away from the Arg120 and shows an orientation that resembles that of the bromo derivative **6e** however projection of the phenyl triazole moiety towards the hydrophilic pocket weakened the binding. Other derivatives carrying lipophilic groups rather than hydrogen bond forming ones (**6a**, **6b** and **6d**) showed hydrophobic interactions with Val523 and failed to form hydrogen bond interaction with Arg120. However, the bi-vinyl containing compound **6d** showed stronger hydrophobic interactions within the active site with its triazole moiety forming a bi CH-π interaction with Leu352 and Val523.

Analysis of the docked **8a-j** compounds revealed that most derivatives bind with their isatin moiety located in the side pocket of COX-2 active site showing a hydrogen bond interaction between the ligand 2-oxo group and Arg513. In addition, the triazole moiety is good fitted between Leu352 and Val523 forming bi CH-π interactions along with the optimized hydrophobic interactions of these compounds to the hydrophobic cleft of the enzyme.

The mono- and dimethoxy substituted derivatives **8h** and **8i** showed almost similar binding modes, although the dimethoxy substituent was better docked within the enzyme pocket. Replacement of methoxy by more polar hydroxy group in compound **8g** decreases the extent of hydrophobic interactions of the whole compound. The methyl substituted derivative **8b** is better bound to the enzyme active site and forms stronger hydrophobic interactions than the unsubstituted ones **8a** and **8d**. The bulky bi-vinyl moiety in compound **8d** induces steric effect resulting in observed shift for the isatin and triazole moieties from their best binding locations within the enzyme pocket (Fig. 3).

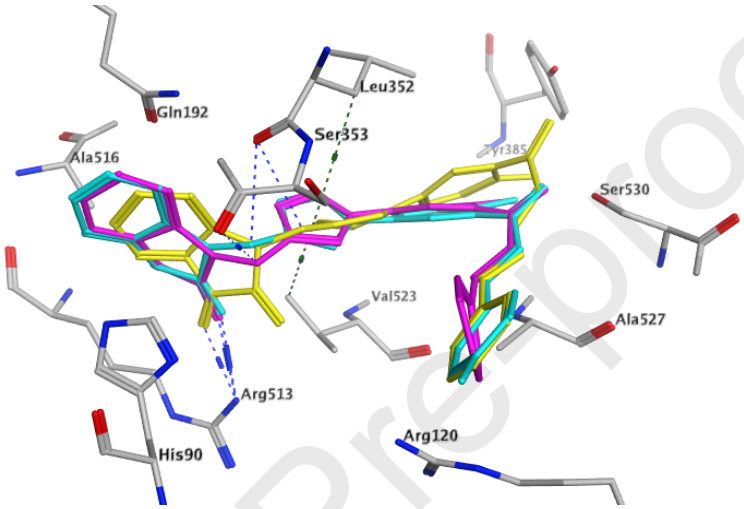

Fig. 3. Docking of compounds **8a** (purple), **8b** (cyan) and **8d** (yellow) into the COX-2 active site showing the effect of the bi-vinyl group on the binding of **8d**.

The same effect was observed with the bulky trimethoxy substituted compound **8j** compared with compounds **8h** and **8j**. The most potent bromo substituted compound **8e** showed better binding interactions and fitting within the active site than the chloro substituted one **8f** which failed to interact with its cholophenyl moiety to Arg513 in the side pocket. Similar to the first series **6a-j**, the moderately active compound **8c** displays different binding mode with its dimethyl amino group located in the side pocket while the 2-oxo of the isatin moiety forms hydrogen bond interaction with Arg120.

2.2.4.2. Docking to 15-LOX

Docking simulations of the new compounds was done and compared with two reference compounds; Quercetin and Zileuton in order to rationalize the biological results of the new compounds. Visualization of the 15-LOX-2 active site revealed that the cavity composed of a hydrophobic hairpin structure where the amino acid residues can adopt an equivalent U-shaped conformation to that of the bound detergent. Also, the crystal structure contains a

catalytic iron Fe^{++} and an apparent channel for invading oxygen lying on opposite sides of the cavity tunnel. This catalytic iron-binding site was found to be coordinated by the imidazole nitrogens of His373, His378, and His553. Mechanistic studies have been demonstrated that iron metal abstracts the hydrogen from the central carbon of the pentadiene and further oxidation also occurs on opposite faces of the amino acid residues [27]. Therefore, the distance between the main phenolic OH of the new compounds and Fe^{++} was measured to give an idea about the proper orientation of the ligand within the active site and the possibility for the compound phenolic OH to be attacked by the enzyme (Table S2).Results indicated that the new compounds **6a-j** and **8a-j** display distances in the range of 5.09 -5.88 Å compared with Quercetin (5.04 Å) and Zileuton (5.12 Å). Overall docking results revealed that all the new compounds showed binding modes within the active site better than that of Quercetin as well as Zileuton (Table S2). The new compounds display binding orientation in the cavity in a U-shaped conformation and are surrounded primarily by the side chains of hydrophobic amino acids. This conformation was adopted as the phenolic OH was found to be capable to form an intramolecular hydrogen bond with its adjacent carbonyl group (Fig. 4).

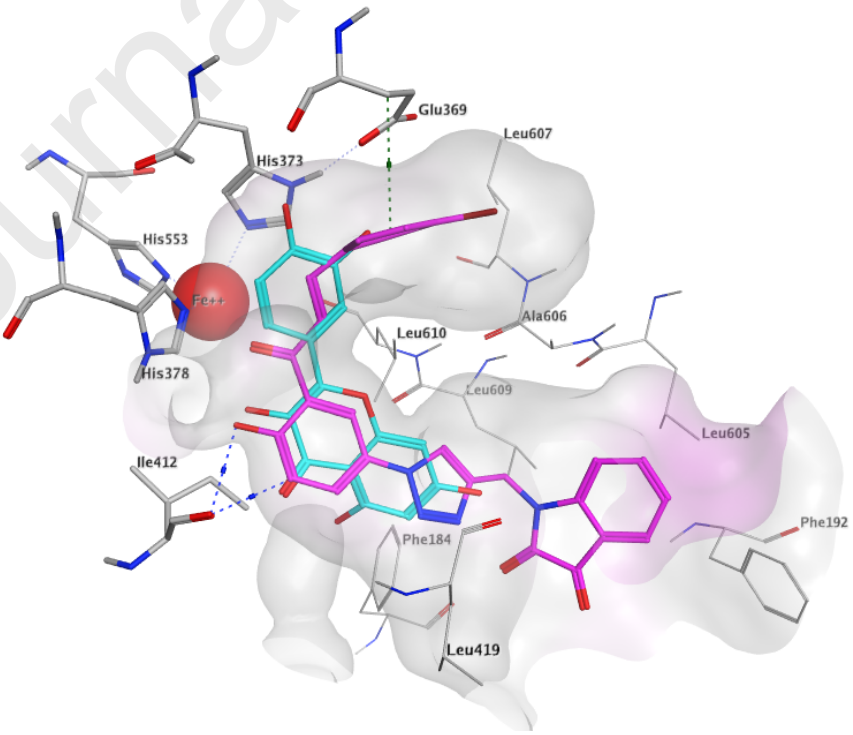

Fig. 4. Docking of compounds **8e** (purple) aligned with Quercetin (cyan) within 15-LOX-2 active site.

Among each series, although being inadequate to find successful correlation between the obtained biological results and the estimated docking within the active site, the analysis could determine some important binding interactions for the new compounds inside the cavity. The main phenolic OH was found to be in the vicinity of the iron metal in a way comparable to that of Quercetin forming hydrogen bond interaction with Ile412 or Asn413. The chalcone moiety occupies the smaller hydrophobic pocket and forms CH-π interaction with the amino acid Glu369 or Leu420. On the other side, the docking analysis revealed that the isatin containing compounds (**8a-j)** showed better binding interactions and filled the cavity of the active site in away better than that displayed by their phenyl congeners (**6a-j)**. Docking of compound **6d** revealed that the compound completely filled the cavity forming strong hydrophobic interactions with the surrounding amino acid residues as well as two hydrogen bond interactions with Ile412 compared with the other lipophilic containing compounds **6a** and **6b**. On the other hand, their congeners **8a**, **8b**, **8d** showed better fitting within the active site owing to the complete fitting of their bulky istain moiety into the larger hydrophobic pocket. For the same reason, the dimethylamino substituted compound **8c** was found to be better oriented within the cavity than its congener **6c** and got stabilized by forming two hydrogen bond interaction with Ile412 rather than Asn413 in addition to the CH-π interactions with Glu369 and Phe184. The halogen containing compounds **6e**, **6f** and their isatin carrying congeners **8e**, **8f** showed almost similar binding modes inside the cavity, however, the chloro substituted compound **8f** displays longer distance from the catalytic Fe^{++} (5.82 Å). Replacing the hydroxyl by methoxy group and even increasing the number of methoxy groups in compounds **6g-j** and **8g-j** has a good effect on the activity. The di- and trimethoxy substituted derivatives **6i** and **6j** showed better binding modes and stronger hydrophobic interactions with the surrounding hydrophobic amino acid residues than the hydroxy and monomethoxy substituted compounds **6g** and **6h** owing to their increased bulkiness within the active site. The same effect could also explain the enhanced potency of

compounds **8g-j** in the order of hydroxy **8g**< monomethoxy **8h**< dimethoxy**8i**< trimethoxy substituted **8j** with their increasing bulkiness inside the cavity hydroxy **8g**< monomethoxy **8h**< dimethoxy**8i**< trimethoxy substituted **8j** (Fig. 5).

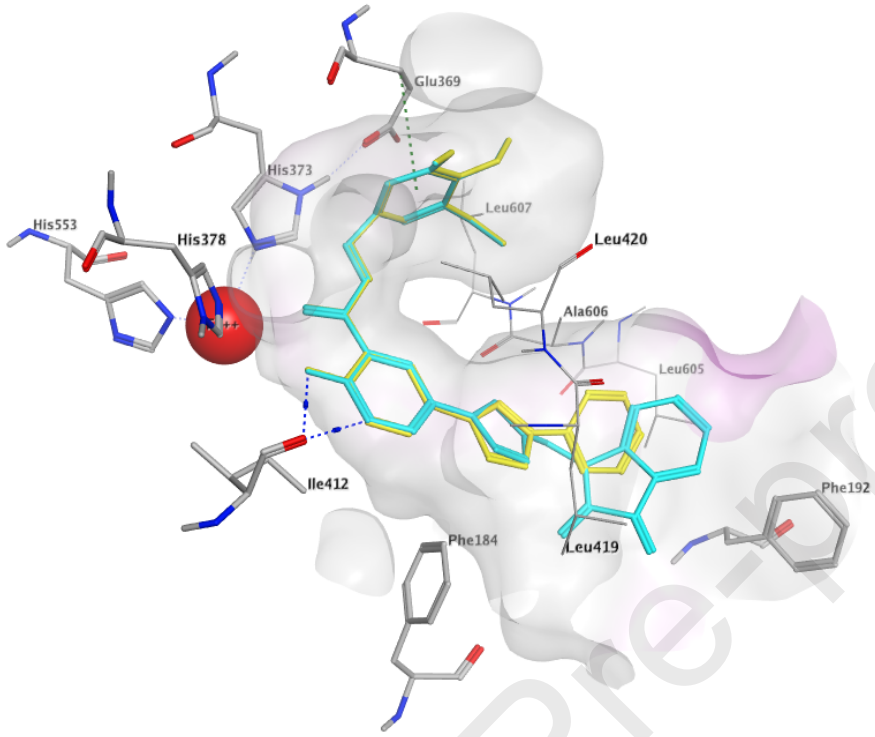

Fig. 5. Docking of compounds **6j** (yellow) aligned with **8j** (cyan) within 15-LOX-2 active site.

3. Conclusion

This study proposed a new rational design of potent anti-inflammatory compounds acting by dual inhibition of COX-2 and 15-LOX. The design is based on combining two or more hybrids having different anti-inflammatory mechanisms; as chalcone – triazole hybrids and chalcone – triazole – isatin hybrids. The obtained results revealed that compounds **6e, 6f, 6i, 8b, 8e** and **8h** showed anti-inflammatory activity equivalent to or even higher than that of celecoxib. *In vitro* COX-1/COX-2 inhibition study revealed that among the synthesized compounds, compound **8h** showed the highest inhibitory activity against COX-2 with an IC_{50} values of 0.037 µM and selectivity index 359.46. Additionally, most compounds showed significant in vitro 15-LOX inhibitory activity higher than that of zileuton. Therefore, compounds **6d**, **6f**, **6i**, **8c**, **8e** and **8h-j** are potent dual inhibitor of COX-2 and 15-LOX. The docking experiments attempted to investigate the binding mode of the final compounds in the binding site of COX-2 and 15-LOX confirmed the high binding selectivity towards COX-2 as well as the difference in activity between different derivatives. Consequently, the *in vitro* and

in vivo anti-inflammatory profiles revealed that these compounds can be a lead for developing new anti-inflammatory drugs.

4. Experimental

4.1. Chemistry

All solvents and reagents used for the synthesis of target compounds were of commercial grade without further purification before use. Melting points were determined on an electrothermal melting point apparatus [Cole-Parmer - Electrothermal IA9100, UK], and were uncorrected. Pre-coated silica gel plates (TLC) (kieselgel 0.25 mm, 60G F254, Merck, Germany) were used for monitoring of the chemical reactions. Spots were detected by using ultraviolet lamp at 254 nm wavelength (Spectroline, model CM-10, USA). (IR) spectra (KBr discs) were recorded on thermo scientific nicolet IS10 FT IR spectrometer (thermo Fischer scientific, USA) at Faculty of science, Assiut University, Assiut, Egypt. ^{1}H-NMR (400 MHz) and ^{13}C-NMR (100 MHz) Spectra were scanned on AVANCE-III High Performance FT-NMR spectrometer, (Brucker Biospin International AG, Swtizerland) at Faculty of Science, Sohag University, Sohag, Egypt except for compounds (**5a-d, 5f, 5h)** which were performed on a Varian EM-390 NMR spectrometer (90 MHz, Varian, CA, USA) at Faculty of Science, Assiut University, Assiut, Egypt, and compounds **6a** and **6b** on AVANCE 500 spectrometer (Bruker Biospin K.K.; Yokohama, Japan). Chemical shifts are expressed in δ-values (ppm) relative to TMS as an internal standard in (90 MHz instrument), using the appropriate solvent as specified. Deuterium oxide was used for the detection of exchangeable protons. Coupling constants (*J*) are reported in Hertz (Hz). ESI-MS were determined using Bruker Daltonics K.K., Yokohama, Japan equipped with electrospray ionization (ESI) interface. Elemental microanalyses were performed on elemental analyzer model flash 2000 thermo fisher at the Regional Center for Mycology and Biotechnology (RCMB), Faculty of Science, Al-Azhar University, Nasr city, Cairo, Egypt.

4.1.1. *N*-(4-Methoxyphenyl)acetamide (1)

To a stirred suspension of *p*-anisidine (6.04 g, 49 mmol) in dichloromethane (20 mL), acetic anhydride (5 mL, 53 mmol) was added over 1 hour. The reaction was stirred for 1 hour more then poured into hexane (60 mL) and stirred for 1 h. The pale grey crystals were filtered, washed with hexane and dried; Yield 7.72 g (95%); mp 128-130 ºC as reported [29].

4.1.2. *N*-(3-Acetyl-4-hydroxyphenyl)acetamide (2):

To a stirred suspension of *N*-(4-methoxyphenyl)acetamide **1** (5.25 g, 32 mmol) and acetyl chloride (6.6 mL, 93 mmol) in dichloromethane (55 mL), aluminum trichloride (14.55 g, 109

mmol) was added portion-wise over 90 min. The reaction was then heated under reflux for 4.5 h and cooled overnight. The reaction mixture was poured into ice then extracted with dichloromethane (5 x 50 mL), dried over $MgSO_4$, filtered and concentrated in vacuo to give the product as green solid that was recrystallized from ethyl acetate - diethyl ether as green crystals. Yield 5.34 g (87%); mp 167-168 ºC as reported [30].

4.1.3. 1-(5-Amino-2-hydroxyphenyl)ethan-1-one (3):

A suspension of *N*-(3-acetyl-4-hydroxy-phenyl)-acetamide **2** (1.03 g, 5.3 mmol) in 15% HCl (1.5 mL, 6.2 mmol) was heated under reflux for 40 min, then cooled and neutralized with 10% aqueous ammonia. The green solid was filtered, washed with water and dried in desiccator. Yield 0.68 g (84%); mp 107-110 ºC as reported [30].

4.1.4. 1-(5-Azido-2-hydroxyphenyl)ethan-1-one (4):

A solution of sodium nitrite (1.46 g, 21.2 mmol) in water (20 mL) was added dropwise to an ice-cold solution of 1-(5-amino-2-hydroxyphenyl)ethan-1-one **3** (2.00 g, 13.2 mmol) in water (100 mL) and conc. H_2SO_4 (15 mL). The reaction mixture was stirred at 0 °C for 30 min. A solution of sodium azide (2.32 g, 35.7 mmol) in water (20 mL) was added dropwise to the mixture. The reaction mixture was further stirred at room temperature for 1h, then gradually cooled to give green crystals, filtered and washed with cooled water and dried in desiccator. Yield 2.25 g (91%); mp 60-61 ºC as reported [23].

4.1.5. (*E*)-1-(5-Azido-2-hydroxyphenyl)-3- substituted prop-2-en-1-ones (5a-j):

Aqueous NaOH (2 mL of 30 g/100 mL) was added to a mixture of **4** (0.5 g, 2.8 mmol) and the appropriate (un)substituted benzaldehyde (3.1 mmol) in ethanol (6 mL), then the reaction mixture was stirred at room temperature for 0.5–12 h. The mixture was neutralized with 15% hydrochloric acid in ice bath. The product was filtered, washed with ethanol, then water, and dried. The formed compounds were crystallized from ethanol–water.

4.1.5.1. (*E*)-1-(5-Azido-2-hydroxyphenyl)-3-phenylprop-2-en-1-one (5a):

Yield 70.1%; mp 121-122 ºC as reported [21]; IR (cm^{-1}, KBr): 3440 (O-H), 3062 (Ar-H), 2114 (N_3) 1646, (C=O), 1576, 1487 (C=C), 692 (=C-H). ^{1}H NMR (90 MHz, δppm $CDCl_3$): 7.0-7.4 (m, 3H, Ar-H), 7.4-7.8 (m, 6H, alkene-H & Ar-H), 8.0 (d, J = 16 Hz, 1H, alkene-H), 13.0 (s, 1H, OH).

4.1.5.2. (*E*)-1-(5-Azido-2-hydroxyphenyl)-3-(*p*-tolyl)prop-2-en-1-one (5b):

Yield 66.8%; mp 100-102 ºC; IR (ύ cm^{-1}, KBr): 3400 (O-H), 3060 (Ar-H), 2920 (C-H aliphatic), 2112 (N_3), 1637 (C=O), 1479, 1561 (C=C), 703 (=C-H). ^{1}H NMR (90 MHz, δ ppm $CDCl_3$): 2.4 (s, 3H, -CH_3), 7.1-7.4 (m, 4H, Ar-H), 7.4-7.6 (m, 4H, alkene-H & Ar-H), 7.9 (d, J = 17 Hz, 1H, alkene-H), 13.0 (s, 1H, OH).

4.1.5.3. (*E*)-1-(5-Azido-2-hydroxyphenyl)-3-(4-(dimethylamino)phenyl)prop-2-en-1-one (5c): Yield 63.3%; mp 128-130 ºC; IR (ύ cm^{-1}, KBr): 3439 (O-H), 3062 (Ar-H), 2911 (C-H aliphatic), 2111 (N_3), 1630 (C=O), 1601 (C=C), 678 (=C-H). ^{1}H NMR (90 MHz, δ ppm $CDCl_3$): 3.98 (s, 6H, N-$(CH_3)_2$), 6.95-7.35 (m, 5H, Ar-H), 7.4-8.1 (m, 4H, alkene-H & Ar-H), 12.95 (s, 1H, OH).

4.1.5.4. (2*E*,4*E*)-1-(5-Azido-2-hydroxyphenyl)-5-phenylpenta-2,4-dien-1-one (5d): Yield 65.4%; mp: >300 ºC; IR (ύ cm^{-1}, KBr): 3423 (O-H); 3027 (Ar-H), 2123 (N_3), 1637 (C=O), 1563, 1483 (C=C), 690 (=C-H). ^{1}H NMR (90 MHz, δ ppm $CDCl_3$): 6.85–7.20 (m, 3H, alkene-H & Ar-H), 7.31-7.67 (m, 6H, alkene-H & Ar-H), 7.73–7.85 (m, 3H, alkene-H & Ar-H), 12.09 (s, 1H, OH).

4.1.5.5. (*E*)-1-(5-Azido-2-hydroxyphenyl)-3-(4-bromophenyl)prop-2-en-1-one (5e): Yield 69.8%; mp 100-102 ºC; IR (ύ cm^{-1}, KBr): 3410 (O-H), 3105 (Ar-H), 2125 (N_3), 1679 (C=O), 1574, 1484 (C=C), 717 (=C-H). ^{1}H NMR (400 MHz, δ ppm $CDCl_3$):7.08 (d, J = 8.8 Hz, 1H, 6'Ar-H), 7.34–7.39 (dd, J = 8.9, 2.7 Hz, 1H, 5'Ar-H), 7.67–7.77 (m, 3H, alkene-H & Ar-H), 7.79–7.89 (m, 3H, alkene-H & Ar-H), 8.00 (d, J = 15.6 Hz, 1H, alkene-H), 12.04 (s, 1H, OH)

4.1.5.6. (*E*)-1-(5-Azido-2-hydroxyphenyl)-3-(4-chlorophenyl)prop-2-en-1-one (5f): Yield 71.0%; mp 113-114 ºC; IR (ύ cm^{-1}, KBr): 3300 (O-H), 3030 (Ar-H), 2115 (N_3), 1644 (C=O), 1582, 1482 (C=C), 718 (=C-H). ^{1}H NMR (90 MHz, δ ppm $CDCl_3$): 7.0-7.35 (m, 3H, Ar-H), 7.4-7.7 (m, 5H, alkene-H & Ar-H), 7.9 (d, J = 16 Hz, 1H, alkene-H), 13.00 (s, 1H, OH).

4.1.5.7. (*E*)-1-(5-Azido-2-hydroxyphenyl)-3-(4-hydroxyphenyl)prop-2-en-1-one (5g): Yield 50.4%; mp >300 ºC; IR (ύ cm^{-1}, KBr): 3450 (O-H), 3079 (Ar-H), 2115 (N_3), 1644 (C=O), 1517, 1482 (C=C), 718 (=C-H). ^{1}H NMR (400 MHz, δ ppm $CDCl_3$): 6.94–7.50 (m, 3H, Ar-H), 7.63–7.94 (m, 2H, alkene-H & Ar-H), 8.03–8.43 (m, 4H, alkene-H & Ar-H), 11.62 (s, 1H, OH), 11.87 (s, 1H, OH).

4.1.5.8. (*E*)-1-(5-Azido-2-hydroxyphenyl)-3-(4-methoxyphenyl)prop-2-en-1-one (5h): Yield 54.3%; mp 130-132 ºC; IR (ύ cm^{-1}, KBr): 3432 (O-H), 3010 (Ar-H), 2837 (C-H aliphatic), 2110 (N_3), 1639 (C=O), 1567, 1512 (C=C), 679 (=C-H). ^{1}H NMR (90 MHz, δ ppm $CDCl_3$): 3.9 (s, 3H, O-CH_3), 6.95-7.2 (m, 3H, Ar-H), 7.25-7.5 (m, 3H, alkene-H & Ar-H), 7.6-8.0 (m, 3H, alkene-H & Ar-H), 13.11 (s, 1H, OH).

4.1.5.9. (*E*)-1-(5-Azido-2-hydroxyphenyl)-3-(3,4-dimethoxyphenyl)prop-2-en-1-one (5i): Yield 50.1%; mp 140-142 ºC; IR (ύ cm^{-1}, KBr): 3400 (O-H), 3060 (Ar-H), 2115 (N_3), 1644 (C=O), 1567, 1512 (C=C), 718 (=C-H). ^{1}H NMR (400 MHz, δ ppm $CDCl_3$): 3.84 (s, 3H, O-

CH_3), 3.87 (s, 3H, O-CH_3), 7.03–7.09 (dd, *J* = 8.5, 6.2 Hz, 2H, Ar-H), 7.36–7.40 (dd, *J* = 8.9, 2.7 Hz, 1H, Ar-H), 7.46 (d, *J* = 8.3 Hz, 1H, Ar-H), 7.55 (s, 1H, Ar-H), 7.77–7.89 (m, 3H, alkene-H & Ar-H), 12.36 (s, 1H, OH).

4.1.5.10. (*E*)-1-(5-Azido-2-hydroxyphenyl)-3-(3,4,5-trimethoxyphenyl)prop-2-en-1-one (5j): Yield 50.2%; mp >300 ºC; IR (ύ cm^{-1}, KBr): 3510 (O-H), 3052 (Ar-H), 2920, 2117 (N_3), 1683 (C=O), 1593, 1486 (C=C), 682 (=C-H). ^{1}H NMR (90 MHz, δ ppm $CDCl_3$): 3.55 (s, 3H, 4-(OCH_3)), 3.64 (s, 6H, 3,5-(OCH_3)), 6.92–7.25 (m, 3H, Ar-H), 7.41–7.96 (m, 4H, alkene-H & Ar-H), 13.51 (s, 1H, OH).

4.1.6. (*E*)-1-(2-Hydroxy-5-(4-phenyl-1*H*-1,2,3-triazol-1-yl)phenyl)-3- substituted prop-2-en-1-ones (6a-j): To a stirred suspension of appropriate derivative of **5a-j (**0.84 mmol) in a mixture of tertiary butanol-water (3:1, 7 mL), phenyl acetylene (0.15 mL, 1.35 mmol) was added. Solutions of sodium ascorbate (33 mg, 0.17 mmol) in water (0.4 mL) and $CuSO_4$. (21 mg, 0.08 mmol) in water (0.3 mL) were added to the stirred mixture at 70 ºC and further stirred overnight. Additional solution of sodium ascorbate (33 mg, 0.17 mmol) in water (0.4 mL) and a solution of $CuSO_4$ (21 mg, 0.08 mmol) in water (0.3 mL) were added and the mixture was further stirred. The reaction progress was monitored by TLC. Water (15 mL) was added and the resultant suspension was stirred for 30 min. the formed precipitate was filtered, washed with water and dried. The products were recrystallized from ethyl acetate-hexane.

4.1.6.1. (*E*)-1-(2-Hydroxy-5-(4-phenyl-1*H*-1,2,3-triazol-1-yl)phenyl)-3-phenylprop-2-en-1-one (6a): Yield 59.9%; yellow solid; mp 202-204 ºC; IR (ύ cm^{-1}, KBr): 3450 (O-H), 3130 (Ar-H), 1644 (C=O), 1575, 1493 (C=C); 692 (Ar-H). ^{1}H NMR (500 MHz, δ ppm $CDCl_3$): 7.19 (d, *J* = 8.9 Hz, 1H, Ar-H), 7.35–7.40 (t, *J* = 7.4 Hz, 1H, Ar-H), 7.43–7.49 (m, 6H, Ar-H), 7.66–7.72 (m, 2H, alkene-H & Ar-H), 7.76-7.80 (dd, *J* = 8.9, 2.5 Hz, 1H, Ar-H), 7.89–7.93 (m, 2H, Ar-H), 8.00 (d, *J* = 15.4 Hz, 1H, alkene-H), 8.39 (s, 1H, triazole-H), 8.40 (d, *J* = 2.5 Hz, 1H, Ar-H), 12.38 (s, 1H, OH). ^{13}C NMR (125 MHz): 117.97, 119.24, 120.00, 120.02, 122.26, 125.88, 128.43, 128.58, 128.70, 129.00, 129.03, 129.16, 130.09, 131.50, 134.17, 147.17, 148.61, 163.66, 193.13 (C=O). ESI-MS (m/z): calcd. (M^++1) 368.1, Found (M^++1) 368.3. Anal. Calcd. for $C_{23}H_{17}N_3O_2$ (367.40): Calculated/Found: 75.19/75.42 (%C), 4.66/4.80 (%H), 11.44/11.69 (%N).

4.1.6.2. (*E*)-1-(2-Hydroxy-5-(4-phenyl-1*H*-1,2,3-triazol-1-yl)phenyl)-3-(*p*-tolyl)prop-2-en-1-one (6b): Yield 57.2%; ; yellow solid; mp 226-228 ºC; IR (ύ cm^{-1}, KBr): 3440 (O-H), 3132 (Ar-H), 2900 (C-H aliphatic), 1644 (C=O), 1577, 1493 (C=C), 691 (Ar-H). ^{1}H NMR

(500 MHz, δ ppm $CDCl_3$): 2.42 (s, 3H, $-CH_3$), 7.19 (d, *J* = 8.9 Hz, 1H, 6'Ar-H), 7.25–7.27 (t, *J* = 3.9 Hz, 2H, 2'',6''Ar-H), 7.37–7.40 (t, *J* = 7.4 Hz, 1H, 4''Ar-H), 7.46–7.49 (t, *J* = 7.6 Hz, 2H, 3'',5''Ar-H), 7.61 (d, *J* = 8.0 Hz, 2H, 3,5Ar-H), 7.65 (d, *J* = 15.4 Hz, 1H, C_b-H), 7.77–7.79 (dd, *J* = 8.9, 2.5 Hz, 1H, 5'Ar-H), 7.93 (d, *J* = 7.2 Hz, 2H, 2,6 Ar-H) 8.00 (d, *J* = 15.3 Hz, 1H, C_a-H) 8.40 (s, 1H, triazole-H) 8.41 (d, *J* = 2.5 Hz, 1H, 3'Ar-H), 13.08 (s, 1H, OH). ^{13}C NMR (125 MHz): 21.67 ($-CH_3$), 117.96, 118.08, 119.69, 120.07, 122.25, 125.87, 128.28, 128.56, 128.64, 128.98, 129.10, 129.90, 130.09, 131.46, 142.32, 147.29, 148.59, 163.65, 193.13 (C=O). ESI-MS (m/z): calcd. (M^++1) 382.1, Found (M^++1) 382.2. Anal. Calcd. for $C_{24}H_{19}N_3O_2$ (381.43): Calculated/Found: 75.57/75.80 (%C), 5.02/5.18 (%H), 11.02/11.34 (%N).

4.1.6.3. (*E*)-3-(4-(Dimethylamino)phenyl)-1-(2-hydroxy-5-(4-phenyl-1*H*-1,2,3-triazol-1-yl)phenyl)prop-2-en-1-one (6c): Yield 55.8%; orange solid; mp 241-243 ºC; IR (ύ cm^{-1}, KBr): 3439 (O-H), 3119 (Ar-H), 2920 (C-H aliphatic), 1634 (C=O), 1550, 1526 (C=C), 695 (Ar-H). ^{1}H NMR (400 MHz, δ ppm DMSO-d_6): 3.05 (s, 6H, $-N(CH_3)_2$), 6.79 (d, *J* = 8.8 Hz, 2H, 3,5 Ar-H), 7.21 (d, *J* = 8.9 Hz, 1H, 6'Ar-H), 7.39–7.43 (t, *J* = 5.8 Hz, 1H, 4''Ar-H), 7.48–7.56 (t, *J* = 7.6 Hz, 2H, 2'',6''Ar-H), 7.77–7.92 (m, 4H, C_a-H & C_b-H & 3'',5''Ar-H), 7.97 (d, *J* = 7.4 Hz, 2H, 2,6 Ar-H), 8.04–8.09 (dd, *J* = 8.9, 2.5 Hz, 1H, 5'Ar-H), 8.58 (d, *J* = 2.5 Hz, 1H, 3'Ar-H), 9.27 (s, 1H, triazole-H), 13.11 (s, 1H, OH). Anal. Calcd. for $C_{25}H_{22}N_4O_2$ (410.47): Calculated/Found: 73.15/73.49 (%C), 5.40/5.47 (%H), 13.65/13.83 (%N).

4.1.6.4. (2*E*,4*E*)-1-(2-Hydroxy-5-(4-phenyl-1*H*-1,2,3-triazol-1-yl)phenyl)-5-phenylpenta-2,4-dien-1-one (6d): Yield 55.7%.; yellow solid; mp 160-162 ºC; IR (ύ cm^{-1}, KBr): 3400 (O-H), 3119 (Ar-H), 1655 (C=O), 1567, 1493 (C=C), 694 (Ar-H). ^{1}H NMR (400 MHz, δ ppm DMSO-d_6): 6.80–7.25 (m, 4H, alkene-H & Ar-H), 7.32-7.64 (m, 8H, alkene-H & Ar-H), 7.70–7.95 (m, 4H, alkene-H & Ar-H), 8.54 (s, 1H, Ar-H), 9.15 (s, 1H, triazole-H), 12.23 (s, 1H, OH). Anal. Calcd. for $C_{25}H_{19}N_3O_2$ (393.44): Calculated/Found: 76.32/76.15 (%C), 4.87/4.98 (%H), 10.68/10.97 (%N).

4.1.6.5. (*E*)-3-(4-bromophenyl)-1-(2-hydroxy-5-(4-phenyl-1*H*-1,2,3-triazol-1-yl)phenyl)-prop-2-en-1-one (6e): Yield 51%.; yellow solid; mp 243-244 ºC; IR (ύ cm^{-1}, KBr): 3448 (O-H), 3133 (Ar-H), 1646 (C=O), 1577, 1489 (C=C), 691 (Ar-H). ^{1}H NMR (400 MHz, δ ppm DMSO-d_6): 7.25 (d, *J* = 7.1 Hz, 1H, Ar-H), 7.41 (d, *J* = 5.2 Hz, 1H, Ar-H), 7.48-7.56 (m, 2H, Ar-H), 7.70 (d, *J* = 6.2 Hz, 2H, Ar-H), 7.81–7.90 (m, 3H, alkene-H & Ar-H), 7.97 (d, *J* = 6.0 Hz, 2H, Ar-H), 8.02–8.12 (m, 2H, alkene-H & Ar-H), 8.53 (s, 1H, Ar-H), 9.25 (s, 1H,

triazole-H), 12.29 (s, 1H, OH). Anal. Calcd. for $C_{23}H_{16}BrN_3O_2$ (446.30): Calculated/Found: 61.90/62.14 (%C), 3.61/3.74 (%H), 9.42/9.73 (%N).

4.1.6.6. (*E*)-3-(4-Chlorophenyl)-1-(2-hydroxy-5-(4-phenyl-1*H*-1,2,3-triazol-1-yl)phenyl)-prop-2-en-1-one (6f): Yield 52.2%; brown solid; mp 230-232 ºC; IR (ύ cm^{-1}, KBr): 3490 (O-H), 3136 (Ar-H), 1639 (C=O), 1582, 1501 (C=C), 691 (Ar-H). ^{1}H NMR (400 MHz, δ ppm DMSO- d_6): 7.24–7.61 (m, 9H, alkene-H & Ar-H), 7.89–7.96 (m, 5H, alkene-H & Ar-H), 9.27 (s, 1H, triazole-H). Microanalysis for $C_{23}H_{16}ClN_3O_2$ (401.85): Calculated/Found: 68.74/69.01 (%C), 4.01/4.13 (%H), 10.46/10.68 (%N).

4.1.6.7. (*E*)-1-(2-Hydroxy-5-(4-phenyl-1*H*-1,2,3-triazol-1-yl)phenyl)-3-(4-hydroxyphenyl) prop-2-en-1-one (6g): Yield 58.6%; yellowish green solid; mp 242-244 ºC; IR (ύ cm^{-1}, KBr): 3400 (O-H), 3133 (Ar-H), 1646 (C=O), 1577, 1494 (C=C), 689 (Ar-H). ^{1}H NMR (400 MHz, δ ppm DMSO-d_6): 7.23 (d, J = 9.7 Hz, 2H, Ar-H), 7.35–7.55 (m, 4H, Ar-H), 7.80-8.35 (m, 7H, alkene-H & Ar-H), 8.45 (s, 1H, Ar-H), 9.28 (s, 1H, triazole-H), 11.93 (s, 1H, OH), 12.13 (s, 1H, OH). Anal. Calcd. for $C_{23}H_{17}N_3O_3$ (383.40): Calculated/Found: 72.05/72.32 (%C), 4.47/4.53 (%H), 10.96/11.12 (%N).

4.1.6.8. (*E*)-1-(2-Hydroxy-5-(4-phenyl-1*H*-1,2,3-triazol-1-yl)phenyl)-3-(4-ethoxyphenyl)-prop-2-en-1-one (6h): Yield 51.2%; yellowish green solid; mp 202-204 ºC; IR (ύ cm^{-1}, KBr): 3400 (O-H), 3130 (Ar-H), 2936 (C-H aliphatic), 1644 (C=O), 1567, 1512 (C=C), 692 (Ar-H). ^{1}H NMR (400 MHz, δ ppm DMSO-d_6): 3.84 (s, 3H, O-CH_3), 7.06 (d, J = 7.6 Hz, 2H, Ar-H), 7.25 (d, J = 7.8 Hz, 1H, Ar-H), 7.38–7.42 (m, 1H, Ar-H), 7.49-7.56 (m, 2H, Ar-H), 7.86-8.00 (m, 6H, alkene-H & Ar-H), 8.09 (d, J = 7.6 Hz, 1H, Ar-H), 8.58 (s, 1H, Ar-H), 9.28 (s, 1H, triazole-H), 12.65 (s, 1H, OH). Anal. Calcd. For $C_{24}H_{19}N_3O_3$ (397.43): Calculated/Found: 72.53/72.80 (%C), 4.82/4.89 (%H), 10.57/10.43 (%N).

4.1.6.9. (*E*)-3-(3,4-Dimethoxyphenyl)-1-(2-hydroxy-5-(4-phenyl-1*H*-1,2,3-triazol-1-yl) phenyl)prop-2-en-1-one (6i): Yield 52.6%; yellow solid; mp 257-259 ºC; IR (ύ cm^{-1}, KBr): 3432 (O-H), 3118 (Ar-H), 2931 (C-H aliphatic), 1640 (C=O), 1568, 1509 (C=C), 695 (Ar-H). ^{1}H NMR (400 MHz, δ ppm DMSO-d_6): 3.84 (s, 3H, O-CH_3), 3.86 (s, 3H, O-CH_3), 7.07 (d, J = 8.3 Hz, 1H, Ar-H), 7.25 (d, J = 8.9 Hz, 1H, Ar-H), 7.37-7.42 (t, J = 7.4 Hz, 1H, Ar-H), 7.49–7.55 (m, 4H, alkene-H & Ar-H), 7.83–7.94 (m, 2H, alkene-H & Ar-H), 7.96 (d, J = 7.7 Hz, 2H, Ar-H), 8.08 (d, J = 8.8 Hz, 1H, Ar-H), 8.54 (s, 1H, Ar-H), 9.28 (s, 1H, triazole-H), 12.56 (s, 1H, OH). Anal. Calcd. for $C_{25}H_{21}N_3O_4$ (427.45): Calculated/Found: 70.25/70.41 (%C), 4.95/4.87 (%H), 9.83/9.98 (%N).

4.1.6.10. (*E*)-1-(2-Hydroxy-5-(4-phenyl-1*H*-1,2,3-triazol-1-yl)phenyl)-3-(3,4,5-trimethoxy

phenyl)prop-2-en-1-one (6j): Yield 49.5%; grey solid; mp 281-283 ºC; IR (ύ cm-^{1}, KBr): 3392 (O-H), 3144 (Ar-H), 2900 (C-H aliphatic), 1731 (C=O), 1495 (C=C), 689 (Ar-H). ^{1}H NMR (400 MHz, δ ppm DMSO- d_6): 3.74 (s, 3H, 4-(OCH_3)), 3.87 (s, 6H, 3,5-(OCH_3)), 7.26–7.51 (m, 6H, Ar-H) 7.80–8.48 (m, 6H, alkene-H & Ar-H), 9.28 (s, 1H, triazole-H), 12.36 (s, 1H, OH). Microanalysis for $C_{26}H_{23}N_3O_5$ (457.48): Calculated/Found: 68.26/68.43 (%C), 5.07/5.14 (%H), 9.19/9.37 (%N).

4.1.7. (*E*)-1-((1-(3-(3-Substituted acryloyl)-4-hydroxyphenyl)-1*H*-1,2,3-triazol-4-yl)methyl)indoline-2,3-diones (8a-j)

To a stirred suspension of appropriate derivative of **5a-j (**1.13 mmol) in a mixture of tertiary butanol-water (3:1, 10 mL), 1-(prop-2-yn-1-yl)-1*H*-indole-2,3-dione **7** [22] (200 mg, 1.08 mmol) was added. Solutions of sodium ascorbate (43 mg, 0.22 mmol) in water (0.4 mL) and $CuSO_4.5H_2O$ (27 mg, 0.11 mmol) in water (0.3 mL) were added and the mixture was stirred at 70 ºC overnight. Additional solution of sodium ascorbate (43 mg, 0.22 mmol) in water (0.4 mL) and a solution of $CuSO_4.5H_2O$ (27 mg, 0.11 mmol) in water (0.3 mL) were added and the mixture was further stirred. The reaction progress was monitored using TLC. Water (20 mL) was added and the resultant suspension was stirred for 30 min. the precipitate formed was filtered, washed with water and dried. Crystallization was performed from dioxane-water.

4.1.7.1. (*E*)-1-((1-(3-Cinnamoyl-4-hydroxyphenyl)-1*H*-1,2,3-triazol-4-yl)methyl)indoline-2,3-dione (8a): Yield 70.2%; yellow solid; mp 245-246 ºC; IR (ύ cm-^{1}, KBr): 3442 (O-H), 3156 (Ar-H), 2990 (C-H aliphatic), 1745, 1644 (C=O), 1497, 1471 (C=C), 696 (Ar-H). ^{1}H NMR (400 MHz, δ ppm DMSO-d_6): 5.09 (s, 2H, CH_2), 7.13–7.26 (m, 3H, Ar-H), 7.35 (d, J = 8.8 Hz, 1H, Ar-H), 7.40–7.52 (m, 3H, Ar-H), 7.56–7.68 (m, 2H, alkene-H & Ar-H), 7.81–8.01 (m, 3H, alkene-H & Ar-H), 8.04–8.15 (m, 1H, Ar-H), 8.40 (s, 1H, Ar-H), 8.87 (s, 1H, triazole-H), 12.27 (s, 1H, OH). Anal. Calcd. For $C_{26}H_{18}N_4O_4$ (450.45): Calculated/Found: 69.33/69.15 (%C), 4.03/4.17 (%H), 12.44/12.80 (%N).

4.1.7.2. (*E*)-1-((1-(4-Hydroxy-3-(3-(*p*-tolyl)acryloyl)phenyl)-1*H*-1,2,3-triazol-4-yl)methyl)indoline-2,3-dione (8b): Yield 71.7 %; yellowish brown solid; mp 253-255 ºC; IR (ύ cm-^{1}, KBr): 3445 (O-H), 3159 (Ar-H), 2921 (C-H aliphatic), 1744, 1643 (C=O), 1579, 1469 (C=C), 682 (Ar-H). ^{1}H NMR (400 MHz, δ ppm DMSO-d_6): 2.38 (s, 3H, -CH_3), 5.09 (s, 2H, CH_2), 7.13 –7.21 (m, 2H, Ar-H), 7.25 (d, J = 8.2 Hz, 1H, Ar-H), 7.31 (d, J = 7.8 Hz, 2H, Ar-H), 7.58–7.70 (m, 2H, alkene-H & Ar-H), 7.78–7.85 (m, 3H, Ar-H), 7.92–8.00 (m, 2H, alkene-H &Ar-H), 8.41 (s, 1H, Ar-H), 8.86 (s, 1H, triazole-H), 12.37 (s, 1H, OH). ^{13}C NMR (100 MHz): 21.63 (-CH_3), 35.53 (CH_2), 111.71, 118.13, 119.47, 122.01, 122.56, 122.74, 122.85, 123.92, 124.98, 128.39, 129.15, 129.78, 130.11, 132.15, 138.63, 138.68, 141.88,

145.88, 150.59, 158.32, 161.16 (C=O), 183.54 (C=O), 193.04 (C=O). Anal. Calcd. for $C_{27}H_{20}N_4O_4$ (464.47): Calculated/Found: 69.82/69.95 (%C), 4.34/4.46 (%H), 12.06/12.31 (%N).

4.1.7.3. (*E*)-1-((1-(3-(3-(4-(Dimethylamino)phenyl)acryloyl)-4-hydroxyphenyl)-1*H*-1,2,3-triazol-4-yl)methyl)indoline-2,3-dione (8c): Yield 69.9%; orange red solid; mp 277-278 ºC; IR (ύ cm^{-1}, KBr): 3448 (O-H), 3144 (Ar-H), 2914 (C-H aliphatic), 1739, 1633 (C=O), 1551, 1494 (C=C), 699 (Ar-H). ^{1}H NMR (400 MHz, δ ppm DMSO-d_6): 3.05 (s, 6H, N-$(CH_3)_2$), 5.10 (s, 2H s, 2H, CH_2), 6.78 (d, *J* = 8.2 Hz, 2H, Ar-H), 7.13-7.19 (m, 2H, Ar-H), 7.26 (d, *J* = 7.7 Hz, 1H, Ar-H), 7.60 (d, *J* = 7.6 Hz, 1H, Ar-H), 7.64–7.90 (m, 6H, alkene-H & Ar-H), 7.96 (d, *J* = 7.5 Hz, 1H, Ar-H), 8.48 (s, 1H, Ar-H), 8.88 (s, 1H, triazole-H), 13.09 (s, 1H, OH). Anal. Calcd. for $C_{28}H_{23}N_5O_4$ (493.51): Calculated/Found: 68.14/68.39 (%C), 4.70/4.82 (%H), 14.19/14.37 (%N).

4.1.7.4.1-((1-(4-Hydroxy-3-((2*E*,4*E*)-5-phenylpenta-2,4-dienoyl)phenyl)-1*H*-1,2,3-triazol-4-yl)methyl)indoline-2,3-dione (8d): Yield 53.4%; brick red solid; mp 232-234 ºC; IR (ύ cm^{-1}, KBr): 3443 (O-H), 3154 (Ar-H), 2852 (C-H aliphatic), 1745, 1638 (C=O), 1570, 1468 (C=C), 682 (Ar-H). ^{1}H NMR (400 MHz, δ ppm DMSO-d_6): 5.08 (s, 2H, CH_2), 7.13–7.24 (m, 3H, alkene-H &Ar-H), 7.29 (d, *J* = 5.4 Hz, 2H, Ar-H), 7.36–7.51 (m, 4H, alkene-H & Ar-H), 7.58-7.69 (m, 5H, alkene-H & Ar-H), 7.97 (d, *J* = 8.7 Hz, 1H, Ar-H), 8.24 (s, 1H, Ar-H), 8.86 (s, 1H, triazole-H), 12.15 (s, 1H, OH). Anal. Calcd. For $C_{28}H_{20}N_4O_4$ (476.48): Calculated/Found: 70.58/70.76 (%C), 4.23/4.36 (%H), 11.76/11.98 (%N).

4.1.7.5. (*E*)-1-((1-(3-(3-(4-Bromophenyl)acryloyl)-4-hydroxyphenyl)-1*H*-1,2,3-triazol-4-yl)methyl)indoline-2,3-dione (8e): Yield 69.3%; yellowish green solid; mp 257-259 ºC; IR (ύ cm^{-1}, KBr): 3380 (O-H); 3158 (Ar-H), 2900 (C-H aliphatic), 1743, 1645 (C=O), 1579, 1489 (C=C), 682 (Ar-H). ^{1}H NMR (400 MHz, δ ppm DMSO-d_6): 5.09 (s, 2H, CH_2), 7.13-7.26 (m, 3H, Ar-H) , 7.60 (d, J = 7.3 Hz, 1H, Ar-H) , 7.64–7.72 (m, 3H, alkene-H & Ar-H) , 7.78-7.88 (m, 3H, alkene-H & Ar-H) , 7.96-8.04 (m, 2H, alkene-H & Ar-H) , 8.40 (s, 1H, Ar-H) , 8.85 (s, 1H, triazole-H), 12.22 (s, 1H, OH). Anal. Calcd. for $C_{26}H_{17}BrN_4O_4$ (529.34): Calculated/Found: 58.99/59.12 (%C), 3.24/3.47 (%H), 10.58/10.81 (%N).

4.1.7.6. (*E*)-1-((1-(3-(3-(4-Chlorophenyl)acryloyl)-4-hydroxyphenyl)-1*H*-1,2,3-triazol-4-yl)methyl)indoline-2,3-dione (8f)

Yield 66.6%; brown solid; mp 228-230 ºC; IR (ύ cm^{-1}, KBr): 3444 (O-H), 3142 (Ar-H), 2943 (C-H aliphatic), 1752, 1735, 1644 (C=O), 1579, 1503 (C=C), 682 (Ar-H). ^{1}H NMR (400 MHz, δ ppm DMSO-d_6): 5.09 (s, 2H, CH_2) , 7.14–7.24 (m, 6H, Ar-H), 7.59–7.68 (m, 3H, alkene-H

& Ar-H) , 7.75–7.90 (m, 2H, alkene-H & Ar-H) , 7.98 (d, *J* = 8.7 Hz, 1H, Ar-H) , 8.35 (s, 1H, Ar-H) , 8.85 (s, 1H, triazole-H), 12.28 (s, 1H, OH). Anal. Calcd. for $C_{26}H_{17}ClN_4O_4$ (484.89): Calculated/Found: 64.40/64.73 (%C), 3.53/3.69 (%H), 11.55/11.86 (%N).

4.1.7.7. (*E*)-1-((1-(4-Hydroxy-3-(3-(4-hydroxyphenyl)acryloyl)phenyl)-1*H*-1,2,3-triazol-4-yl)methyl)indoline-2,3-dione (8g)

Yield 71.9%; reddish brown solid; mp 244-246 ºC; IR (ύ cm^{-1}, KBr): 3458 (O-H), 3081 (Ar-H), 2926 (C-H aliphatic), 1735, 1645 (C=O), 1576, 1470 (C=C), 700 (=C-H). ^{1}H NMR (400 MHz, δ ppm DMSO- d_6): 5.09 (s, 2H, CH_2), 7.13–7.23 (m, 3H, Ar-H), 7.58-7.69 (m, 2H, alkene-H & Ar-H), 7.87 (d, *J* = 15.7 Hz, 1H, alkene-H), 7.96–8.01 (dd, *J* = 8.5, 2.0 Hz, 1H, Ar-H), 8.08–8.16 (m, 3H, alkene-H & Ar-H), 8.31 (d, *J* = 8.6 Hz, 2H, Ar-H), 8.37 (d, *J* = 1.9 Hz, 1H, Ar-H), 8.85 (s, 1H, triazole-H), 12.03 (s, 1H, OH). Anal. Calcd. for $C_{26}H_{18}N_4O_5$ (466.44): Calculated/Found: 66.95/66.80 (%C), 3.89/3.97 (%H), 12.01/12.24 (%N).

4.1.7.8. (*E*)-1-((1-(4-Hydroxy-3-(3-(4-methoxyphenyl)acryloyl)phenyl)-1*H*-1,2,3-triazol-4-yl)methyl)indoline-2,3-dione (8h): Yield 64%; red solid; mp 274-276 ºC; IR (ύ cm^{-1}, KBr): 3400 (O-H), 3159 (Ar-H), 2921 (C-H aliphatic), 1744, 1643 (C=O), 1579, 1469 (C=C), 682 (=C-H). ^{1}H NMR (400 MHz, δ ppm DMSO-d_6): 3.85 (s, 3H, O-CH_3), 5.09 (s, 2H, CH_2), 7.05 (d, *J* = 8.5 Hz, 2H, Ar-H), 7.13–7.20 (m, 2H, Ar-H), 7.25 (d, *J* = 8.1 Hz, 1H, Ar-H), 7.58–7.70 (m, 2H, alkene-H & Ar-H), 7.85–7.90 (m, 4H, alkene-H &Ar-H), 7.95–7.99 (dd, *J* = 8.7, 1.9 Hz, 1H, Ar-H), 8.44 (d, *J* = 1.9 Hz, 1H, Ar-H), 8.86 (s, 1H, triazole H), 12.53 (s, 1H, OH). Anal. Calcd. for $C_{27}H_{20}N_4O_5$ (480.47): Calculated/Found: 67.49/67.65 (%C), 4.20/4.37 (%H), 11.66/11.49 (%N).

4.1.7.9. (*E*)-1-((1-(3-(3-(3,4-Dimethoxyphenyl)acryloyl)-4-hydroxyphenyl)-1*H*-1,2,3-triazol-4-yl)methyl)indoline-2,3-dione (8i): Yield 67.7 %; yellowish green solid; mp 211-212 ºC; IR (ύ cm^{-1}, KBr): 3447 (O-H), 3080 (Ar-H), 2936 (C-H aliphatic), 1740, 1640 (C=O), 1571, 1511 (C=C), 711 (=C-H). ^{1}H NMR (400 MHz, δ ppm DMSO-d_6): 3.84 (s, 6H, -OCH_3), 5.09 (s, 2H, , CH_2) , 7.05 (d, *J* = 7.6 Hz, 1H, Ar-H) , 7.12–7.28 (m, 4H, Ar-H), 7.42–7.53 (m, 2H, alkene-H & Ar-H) , 7.58–7.70 (m, 2H, alkene-H & Ar-H) , 7.78–7.90 (m, 2H, alkene-H & Ar-H) , 7.98 (d, *J* = 7.9 Hz, 1H, Ar-H) , 8.41 (s, 1H, Ar-H) , 8.86 (s, 1H, triazole-H) , 12.51 (s, 1H. OH). Anal. calcd. for $C_{28}H_{22}N_4O_6$ (510.50): Calculated/Found: 65.88/66.12 (%C), 4.34/4.48 (%H), 10.97/11.18 (%N).

4.1.7.10. (*E*)-1-((1-(4-Hydroxy-3-(3-(3,4,5-trimethoxyphenyl)acryloyl)phenyl)-1*H*-1,2,3-triazol-4-yl)methyl)indoline-2,3-dione (8j): Yield 63.3 %; brown solid; mp 267-269 ºC; IR (ύ cm^{-1}, KBr): 3420 (O-H), 3071 (Ar-H), 2919 (C-H aliphatic), 1739, 1614 (C=O), 1493 (C=C), 762 (Ar-H). ^{1}H NMR (400 MHz, δ ppm DMSO-d_6): 3.55 (s, 3H, 4-(OCH_3)), 3.73 (s,

6H, 3,5-(OCH_3)), 5.06 (s, 2H, CH_2), 7.13–7.24 (m, 2H, Ar-H), 7.33–7.48 (m, 3H, Ar-H), 7.55–7.69 (m, 4H, alkene-H & Ar-H), 7.85–7.95 (m, 2H, alkene-H & Ar-H), 8.79 (s, 1H, triazole-H), 13.22 (s, 1H, OH). Anal. calcd. for $C_{29}H_{24}N_4O_7$ (540.52): Calculated/Found: 64.44/64.81 (%C), 4.48/4.59 (%H), 10.37/10.59 (%N).

4.2. Biology

4.2.1. *In vitro* cyclooxygenase inhibition assay

Cyclooxygenase inhibition studies were carried out at the department of Biochemistry, Faculty of Medicine, Cairo University, Cairo, Egypt. Synthesized compounds were tested for their ability to inhibit ovine COX-1 and human recombinant COX-2 using a COX inhibitor screening assay kit (Catalog No. 560131, Cayman Chemical, Ann Arbor, MI, USA) according to the manufacturer's instructions and the deviation from the mean is < 10% of the mean value.

4.2.2. *In vitro* lipoxygenase inhibition assay

Lipoxygenase inhibition studies were carried out at the department of Biochemistry, Faculty of Medicine, Cairo University, Cairo, Egypt. Synthesized compounds tested for their ability to inhibit LOX enzyme using LOX inhibitor screening assay kit (Catalog No. 760700, Cayman Chemical, Ann Arbor, MI, USA) according to the manufacturer's instructions and the deviation from the mean is < 10% of the mean value

4.2.3. *In vivo* Anti-inflammatory activity by carrageenan induced paw edema method

The *in vivo* anti-inflammatory activity of the selected compounds (**6e, 6f, 8b, 8e** and **8h**) were tested by carrageenan induced paw edema method [31] in rats in comparison to Celecoxib® as a reference drug. The test is based on the pedal inflammation in rat paws induced by subplantar injection of carrageenan suspension (0.2 mL of 1% solution in normal saline) into the right hind paw of the rats. Male adult albino rats (120–150 g) were divided into groups, each of five animals. The thickness of rat paw was measured by a Vernier calliper (SMIEC, China) before and 30 min after carrageenan injection to detect the carrageenan induced inflammation. Each test compound at a dose of 28 μmol/Kg (dissolved in 1% sodium carboxymethyl cellulose solution in normal saline) was injected i.p. to different groups of rats. Control group received a vehicle (1% sodium carboxymethyl cellulose solution in normal saline), while the two reference groups received Celecoxib and Diclofenac sodium i.p. at the same dose of the tested compounds. The difference between the thicknesses of the two paws was taken as a measure of edema. The measurement was carried out at 1, 2, 3 and 4 h after injection of the test compounds, reference drugs. The percentages of edema inhibition were calculated according to the following equation. Two-way ANOVA followed by

Dunnett's multiple comparisons test was performed using GraphPad Prism version 7.00 for Windows, GraphPad Software, La Jolla California USA.

$$\% \text{ Edema inhibition} = \frac{(V_R - V_L)\ \text{control} - (V_R - V_L)\ \text{treated}}{(V_R - V_L)\ \text{control}} \times 100$$

where VR: Average right paw thickness, VL: Average left paw thickness.

4.2.4. Docking and Molecular Modeling

Molecular modeling studies was carried out at the department of medicinal chemistry, faculty of pharmacy, Assiut University, Assiut, Egypt. All the molecular modeling calculations and docking simulation studies were performed on a Processor Intel(R) Pentium (R) CPU N3510@ 1.99GHz and 4 GB Memory with Microsoft Windows 8.1 pro (64 Bit) operating system using Molecular Operating Environment (MOE 2014.0901, 2014; Chemical Computing Group, Canada) as the computational software.

All MOE minimizations were performed until a RMSD gradient of 0.01 Kcal/mol/A with the forcefield (MMFF94) to calculate the partial charges automatically. The Alpha Triangle placement was chosen to derive the poses by random superposition of ligand atom triplets through alpha sphere dummies in the receptor site. The London ΔG scoring function estimates the free energy of binding of the ligand from a given pose. Refining the results was completed using the MMFF94 forcefield, and rescoring of the refined results using the London ΔG scoring function was applied. The output database dock file was created with different poses for each ligand and arranged according to the final score function (S), which is the score of the last stage that was not set to zero.

Acknowledgements

This work was supported by Faculty of pharmacy, Assiut University.

Declaration of Competing Interest

The authors have declared no conflict of interest

Supplementary material

Supplementary data to this article can be found online at …….

References

[1] M. Karin, H. Clevers, Reparative inflammation takes charge of tissue regeneration,

Nature 529 (2016) 307-315.

[2] A. Lannergård, A. Larsson, P. Kragsbjerg, G. Friman, Correlations between serum amyloid A protein and C-reactive protein in infectious diseases, Scand. J. Clin. Lab. Investigat. 63 (2003) 267-272.

[3] T. Zebardast, A. Zarghi, B. Daraie, M. Hedayati, O.G. Dadrass, Design and synthesis of 3-alkyl-2-aryl-1,3-thiazinan-4-one derivatives as selective cyclooxygenase (COX-2) inhibitors, Bioorg. Med. Chem. Lett. 19 (2009) 3162–3165.

[4] L.J. Crofford, Use of NSAIDs in treating patients with arthritis, Arthritis. Res. Ther. 15 (2013) S2.

[5] C. Zhuang, W. Zhang, C. Sheng, W. Zhang, C. Xing, Z. Miao, Chalcone: A Privileged Structure in Medicinal Chemistry, Chem. Rev. 117 (2017) 7762-7810.

[6] H. Ur Rashid, Y. Xu, N. Ahmad, Y. Muhammad, L. Wang, Promising anti-inflammatory effects of chalcones via inhibition of cyclooxygenase, prostaglandin E_2, inducible NO synthase and nuclear factor κB activities, Bioorg. Chem. 87 (2019) 335- 365.

[7] A. Detsi, M. Majdalani, C.A. Kontogiorgis, D. Hadjipavlou-Litina, P. Kefalas, Natural and synthetic 2'-hydroxy-chalcones and aurones: synthesis, characterization and evaluation of the antioxidant and soybean lipoxygenase inhibitory activity, Bioorg. Med. Chem. 17 (2009) 8073-8085.

[8] S. Sogawa, Y. Nihro, H. Ueda, A. Izumi, T. Miki, H. Matsumoto, T. Satoh,3,4-Dihydroxychalcones as Potent 5-Lipoxygenase and Cyclooxygenase Inhibitors, J. Med. Chem. 36 (1993) 3904-3909.

[9] R. Sribalan, G. Banuppriya, M. Kirubavathi,A. Jayachitra,V. Padmini, Multiple biological activities and molecular docking studies of newly synthesized 3-(pyridin-4-yl)-1H-pyrazole-5-carboxamide chalcone hybrids, Bioorg. Med. Chem. Lett. 26 (2016) 5624-5630.

[10] M. Pal, N.K. Sharma, K.K. Priyanka, Synthetic and biologic multiplicity of isatin, J. Adv. Sci. Res. 2 (2011) 35-44.

[11] S.K. Seshaiah, A. Ramesh, Synthesis and pharmacological activities of hydrazones, Schiff and Mannich bases of isatin derivatives, Biol. Pharm. Bull. 24 (2001) 149-52.

[12] M.E. Matheus, F.D.A. Violante, S.J. Garden, A.C. Pinto, Isatin inhibit cyclooxygenase-2 and inducible nitric oxide synthase in a mouse macrophage cell-line, Eur. J. Pharmcol. 556 (2007)200-206.

[13] A. Sahu, D. DasRam, K. Agrawal, A. Gajbhiye, Bio-isosteric replacement of amide

group with 1,2,3-triazole in phenacetin improves the toxicology and efficacy of phenacetin-triazole conjugates, Life Sci. 228 (2019) 176-188.

[14] A.K. Kumara, V. Sunithaa, B. Shankara, M. Ramesha, T.M. Krishnab, P. Jalapathi, Synthesis, biological evaluation, and molecular docking studies of novel 1,2,3-triazole derivatives as potent anti-inflammatory agents, Russian J. Gen. Chem. 86 (2016) 1154–1162.

[15] T.W. Kim, Y. Yong, S.Y. Shin, H. Jung, K.H. Park, Y.H. Lee, Y. Lim, K.Y. Jung, Synthesis and biological evaluation of phenyl-1H-1,2,3-triazole derivatives as anti-inflammatory agents, Bioorg. Chem. 59 (2015) 1-11.

[16] F. Naaza, M.C. PreetiPallavib, S. Shafic, N. Mulakayalad, M.S. Yara, H.M. Sampath Kumar, 1,2,3-triazole tethered Indole-3-glyoxamide derivatives as multiple inhibitors of 5-LOX, COX-2 & tubulin: Their anti-proliferative & anti-inflammatory activity, Bioorg. Chem. 81 (2018) 1-20.

[17] C. Viegas-Junior, A. Danuello, V. da Silva Bolzani, E.J. Barreiro, C.A.M. Fraga, Molecular hybridization: a useful tool in the design of new drug prototypes, Curr.Med. Chem. 14 (2007) 1829-1852.

[18] J. Zhou, X. Jiang, S. He, H. Jiang, F. Feng, W. Liu, W. Qu, H. Sun, Rational Design of Multitarget-Directed Ligands: Strategies and Emerging Paradigms, J. Med. Chem. (2019) doi: 10.1021/acs.jmedchem.9b00017.

[19] H.A. Abou-Zied, B.G.M. Youssif, M.F.A. Mohamed, A.M. Hayallah, M. Abdel-Aziz, EGFR inhibitors and apoptotic inducers: Design, synthesis, anticancer activity and docking studies of novel xanthine derivatives carrying chalcone moiety as hybrid molecules, Bioorg. Chem. 89 (2019) 102997. doi: 10.1016/j.bioorg.2019.102997.

[20] Y.M. Omar, H.H.M. Abdu-Allah, S.G. Abdel-Moty, Synthesis, biological evaluation and docking study of 1,3,4-thiadiazole-thiazolidinone hybrids as anti-inflammatory agents with dual inhibition of COX-2 and 15-LOX, Bioorg. Chem. 2018, 80C, 461-471.

[21] H.H.M. Abdu-Allah, B.G.M. Youssif, M. Abd-Elrhman, M. Abdel-Hamid, R. Reshma, P. Yogeeswari, T. Aboul-Fadl, D. Sriram, Synthesis and anti-mycobacterial activity of 4-(4-phenyl-1H-1,2,3-triazol-1-yl)salicylhydrazones: revitalizing an old drug, Arch. Pharm. Res. 40 (2017) 168-179.

[22] H.H.M. Abdu-Allah, S.G. Abdel-Moty, R. El-Awady, A.A. El-Shorbagi, Design and synthesis of novel 5-aminosalicylate (5-ASA)-4-thiazolinone hybrid derivatives with promising antiproliferative activity, Bioorg. Med. Chem. Lett. 26 (2016) 1647-1650.

[23] S. Yap, O.L. Woodman, P.J. Crack, S.J. Williams, Synthesis of a hypoxia-targeted conjugate of the cardioprotective agent 3',4'-dihydroxyflavonol and evaluation of its ability to reduce ischaemia/reperfusion injury, Bioorg. Med. Chem. Lett. 21 (2011) 5102-5106.

[24] S. Shafi, M.M. Alam, N. Mulakayala, C. Mulakayala, G. Vanaja, A.M. Kalle, R. Pallu, M.S. Alam, Synthesis of novel 2-mercapto benzothiazole and 1,2,3-triazole based bis-heterocycles: their anti-inflammatory and anti-nociceptive activities, Eur. J. Med. Chem. 49 (2012) 324-333.

[25] Molecular Operating Environment (MOE), 2014.0901; Chemical Computing Group Inc., 1010 Sherbooke St. West, Suite #910, Montreal, QC, Canada, H3A 2R7, 2016.

[26] B.J. Orlando, M.G. Malkowski, Crystal Structure of Rofecoxib Bound to Human Cyclooxygenase-2. Acta Crystallogr. Sect. F Struct. Biol. Commun. 72 (2016) 772–776.

[27] M.K. Kobe, D.B. Neau, C.E. Mitchell, S.G. Bartlett, M.E. Newcomer, the Structure of human 15-lipoxygenase-2 with a substrate mimic. J. Biol. Chem. 289 *(*2014), 8562–8569.

[28] R.G. Kurumbail, A.M. Stevens, J.K. Gierse, J.J. McDonald, R.A. Stegeman, J.Y. Pak, D. Gildehaus, J.M. Miyashiro, T.D. Penning, K. Seibert, P.C. Isakson, W.C. Stallings, structural basis for selective inhibition of cyclooxygenase-2 by anti-inflammatory agents, *Nature* 384 (1996) 644–648.

[29] N. Maraš, S. Polanc, M. Kočevar, Microwave-assisted methylation of phenols with tetramethylammonium chloride in the presence of K_2CO_3 or Cs_2CO_3, Tetrahedron 64 (2008) 11618-11624.

[30] C.T. Chang, F.C. Chen, T.S. Chen, K.K. Hsu, T. Ueng, M. Hung, Synthesis of 6-halogenoflavones and related compounds, J. Chem. Soc. (Resumed) (1961) 3414-3417.

[31] L.V.G. Nargund, G.R.N. Reddy, V. Hariprasad, Anti-inflammatory activity of substituted 1,3,4-oxadiazoles, J. Pharm. Sci. 83 (1994) 246-248.

Declaration of Competing Interest

The authors have declared no conflict of interest

Graphical abstract

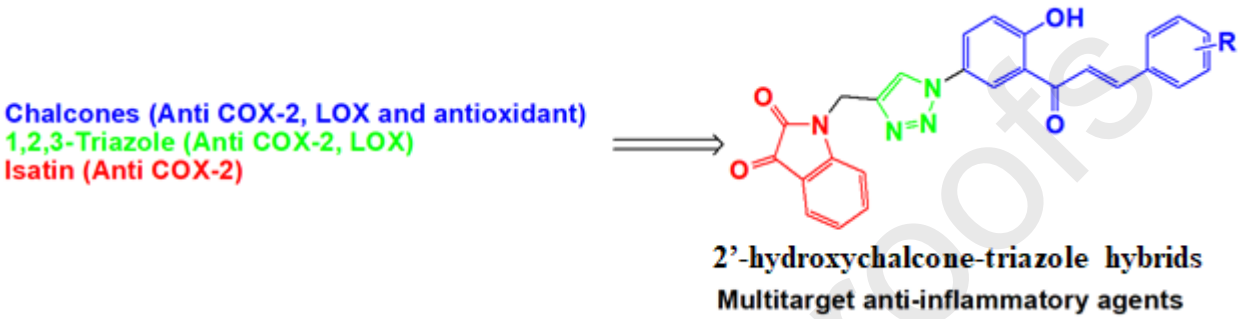

Highlights

1. The efficient synthesis of the privileged multifunctional intermediate 5-azido-2-hydroxyacetophenone

2. The synthesis of 20 new 2'-hydroxychalcone-triazole hybrids some endowed with isatin

3. Six compounds showed promising *in vivo* anti-inflammatory activity with potent dual inhibition of COX-2 and 15-LOX and could be used as lead compounds for developing anti-inflammatory agents.

4. Molecular docking studies disclosed important binding modes with COX-2 and 15-LOX.